CrystEngComm

Accepted Manuscript

ROYAL SOCIETY OF CHEMISTRY

www.rsc.org/crystengcomm

Cite this: DOI: 10.1039/c0xx00000x

www.rsc.org/xxxxxx

ARTICLE TYPE

Crystal Engineering of Homochiral Molecular Organization of Naproxen in Cocrystals and Their Thermal Phase Transformation Studies

K. Manoj,* Rui Tamura, Hiroki Takahashi and Hirohito Tsue

Received (in XXX, XXX) Xth XXXXXXXXX 20XX, Accepted Xth XXXXXXXXX 20XX
DOI: 10.1039/b000000x

Since the racemic naproxen does not have the desired crystal structure essential to induce preferential enrichment, we used crystal engineering principle to produce the required homochiral *R*- and *S*-chains in the solid state. The cocrystal structures of racemic and *S*-naproxen (NPX) with bipyridine (BPY) and piperazine (PIZ) were determined, which consist of homochiral 1D naproxen chains that are associated by weak non-covalent interactions. Thermal studies of both racemic and *S*-naproxen–bipyridine cocrystals indicated a monotropic polymorphic transformation upon heating and the new crystalline phase was characterized by DSC, PXRD, hot-stage microscopy, and FT-IR spectroscopy.

Introduction

Crystal engineering is the rational design of functional molecules with targeted properties by utilizing the knowledge of non-covalent interactions for the assembly of crystalline materials.[1] Recently, crystal engineering has gained great importance in pharmaceutical industries because of its utility for the improved physico-chemical properties of active pharmaceutical ingredients (API) by co-crystallization.[2] Pharmaceutical cocrystals[3] can provide a straightforward way to change the solid state properties such as solubility, mechanical compressibility and thermal or photochemical stability.[4] The primary design strategy for constructing a new cocrystal needs the understanding of the intermolecular interactions such as hydrogen bonds,[5] halogen bonding,[6] dipole–dipole[7] or other weak non-covalent interactions[8] that prevail in the molecular crystals. However, there is still considerable uncertainty that a given cocrystal will be formed or not, which depends on the various aspects of thermodynamic or kinetic nature of crystallization.[9] A cocrystal can be successfully prepared by exploring the various experimental techniques[10] such as crystallization from various solvents[11] or the melt, or by solvent-drop grinding,[12] or using lattice energy calculation to investigate whether a particular cocrystal is thermodynamically stable than their individual crystals.[13]

Graduate School of Human and Environmental Studies, Kyoto University, Kyoto-606-8501, Japan. E-mail:k.manoj.chem@gmail.com; Fax: +81-75-753-7915 Tel: +81-75-753-2970

† Electronic Supplementary Information (ESI) available: (i) geometrical parameters of significant intermolecular interactions, (ii) molecular layer figure of *RS*-naproxen viewing down the *a*-axis (iii) molecular layer figures of cocrystals viewing down the *a*-axis and (iv) combined DSC plots of cocrystals and their individual components. CCDC reference numbers 931856–931859. See http://dx.doi.org/10.1039/b000000x/

Preferential enrichment is a unique, chiral symmetry-breaking spontaneous enantiomeric resolution phenomenon exhibited by a certain kind of racemic mixed crystals (or solid solution) under non-equilibrium crystallization conditions.[14] Using this technique, we have successfully resolved the enantiomers of various amino acids[15] and ketoprofen,[16] which satisfied all the five requirements[17] for the occurrence of preferential enrichment. In order to extend the scope of preferential enrichment to the other profen drugs, naproxen was chosen, which is one of the most widely used non-steroidal anti-inflammatory drugs (NSAID) and the bioactivity of naproxen is essentially associated with the *S*-enantiomer.[18] The crystal structure of racemic naproxen was determined by PXRD and computational methods[19] due to the difficulty in obtaining suitable single crystals (although we solved the single crystal X-ray structure and deposited data to the CSD; No.858772) and it does not have the required molecular structure (*see supporting information for molecular packing, SF1*) essential to induce preferential enrichment. Therefore, crystal engineering principles were applied for achieving the desired molecular organization consisting of homochiral *R*- and *S*-chains of naproxen in naproxen–bipyridine (NPX–BPY) and naproxen–piperazine (NPX–PIZ) cocrystals (Chart 1).

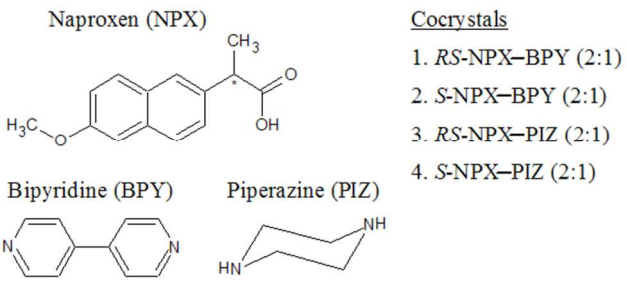

Chart 1

Experimental Section

General

Commercially available *RS*-naproxen, *S*-naproxen, bipyridine and piperazine have been used without further purification. The IR spectra were recorded on a Shimadzu IR Prestige-21 spectrophotometer with sample on KBr pellet and ^{1}H NMR spectra measured on JEOL JNM-A500 instrument. Hot stage microscopic (HSM) images of phase transformations were captured on Olympus BH2 microscope equipped with heating control unit TH-600PH.

Cocrystal Preparation

The naproxen–bipyridine cocrystals were prepared by mixing a 2:1 stoichiometric ratio of *RS*- or *S*-naproxen (1.150 g) and bipyridine (0.390 g) in methanol (10 mL) and dissolved completely by heating at 60°C, followed by slow evaporation at room temperature in the absence of light. Colourless plate crystals of NPX–BPY were obtained after 24h (1.413 g, 92%). Similarly, a 2:1 ratio of *RS*- or *S*-naproxen (1.150 g) and piperazine (0.215 g) were dissolved completely in 12 mL methanol-water (2:1) mixture, warmed, and kept at room temperature; colourless block crystals of NPX–PIZ were formed after 12h (1.287 g, 94%).

Differential Scanning Calorimetry (DSC)

DSC measurements were performed on a Shimadzu DSC-60 instrument. About 2-3 mg of the cocrystals were placed in an aluminium pan and heated at a rate of 5°C/min. An empty pan was used as the reference and dry nitrogen used for purging (30 mL/min). The phase transformation studies of naproxen–bipyridine cocrystals were carried out by heating the sample from 30°C to 165°C, then cooled to 30°C and repeated the experiment by heating and cooling at a rate of 5°C/min. The melting peak for the cocrystals of *RS*-NPX–BPY, *S*-NPX–BPY, *RS*-NPX–PIZ and *S*-NPX–PIZ was found to be 135°C, 119°C, 218°C and 213°C, respectively (Fig.1)

Single Crystal X-Ray Diffraction (SCXRD)

X-ray intensity data were collected on a Rigaku Saturn 724+ CCD diffractometer in omega and phi scan mode, $\lambda_{MoK\alpha}$ = 0.71073 Å at low temperature (173 K). All the intensities were corrected for Lorentzian, polarization and absorption effects using Rigaku *CrystalClear* software.[20] The crystal structures were solved by *Direct* methods using program *SIR-97*[21] and the full-matrix least squares refinements on F^2 were carried out by using *SHELXL-97*.[22] All non-hydrogen atoms were refined anisotropically, and hydrogen atoms were placed in idealized positions and constrained to ride on their parent atoms. Molecular graphics were generated using *Mercury*[23] software. Table 1 summarizes the crystallographic details of naproxen cocrystals. All the crystal data (931856-931859) have been deposited with

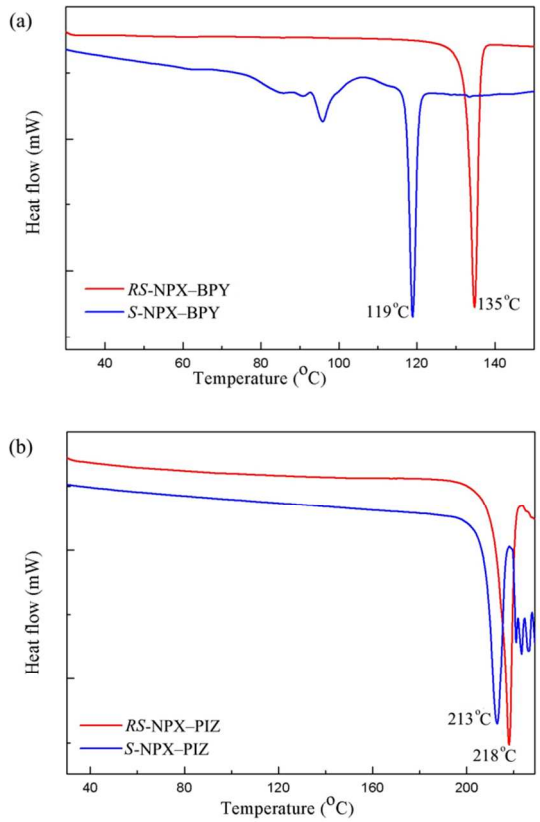

Fig. 1 DSC plots of (a) naproxen–bipyridine and (b) naproxen–piperazine cocrystals.

Table 1: Summary of crystallographic details of naproxen cocrystals.

	RS-NPX–BPY	*S*-NPX–BPY	*RS*-NPX–PIZ	*S*-NPX–PIZ
Chemical formula	$C_{14}H_{14}O_3$, 0.5 ($C_{10}H_8N_2$)	2($C_{14}H_{14}O_3$), $C_{10}H_8N_2$	$C_{14}H_{14}O_3$, 0.5 ($C_4H_{10}N_2$)	2($C_{14}H_{14}O_3$), $C_4H_{10}N_2$
M_r	308.34	616.69	272.31	544.63
Crystal size	0.30×0.10×0.09	0.17×0.11×0.04	0.32×0.07×0.06	0.21×0.08×0.05
Crystal system, space group	Monoclinic, $P2_1/c$	Monoclinic, $P2_1$	Monoclinic, $P2_1/c$	Monoclinic, $P2_1$
a /Å	7.7624(6)	15.206(6)	7.966(4)	8.029(4)
b /Å	5.800(4)	5.766(2)	6.012(3)	6.118(3)
c /Å	36.02(3)	19.370(8)	28.985(15)	28.045(14)
β /°	90.017(8)	111.189(5)	91.739(7)	93.990(7)
V /Å^3	1593.5(2)	1583.5(11)	1387.5(12)	1374.3(12)
Z, D_{calc}/g cm^{-3}	4, 1.286	2, 1.293	4, 1.304	2, 1.316
μ /mm^{-1}, F(000)	0.087, 652	0.088, 652	0.090, 580	0.091, 580
Absorption correction, θ_{max}/°	Multi-scan, 26.00	Multi-scan, 27.46	Multi-scan, 27.46	Multi-scan, 27.47
h, k, l (min, max)	(-9,9),(-7,7), (-43,44)	(-19,19), (-7,7), (-25,25)	(-5,10), (-7,7), (-37,35)	(-8,10), (-7,7), (-36,23)
Reflns collected, unique, observed	13044, 3089, 2359	14102, 7113, 4073	6743, 3120, 1755	7649, 5112, 2996
No. of parameters	229	417	203	365
R_{int}	0.0704	0.0547	0.0447	0.0584
$R_1[I > 2\sigma(I)]$, R_1_all data	0.0965, 0.1846	0.0753, 0.1402	0.0928, 0.1627	0.0799, 0.1382
$wR_2[I > 2\sigma(I)]$, wR_2_all data	0.1270, 0.1980	0.1128, 0.1353	0.1671, 0.1936	0.1360, 0.1670
GoF	1.189	1.008	1.101	1.021
$\Delta\rho_{max}$, $\Delta\rho_{min}$/eÅ^{-3}	0.536, –0.317	0.199, –0.207	0.338, –0.346	0.375, –0.418

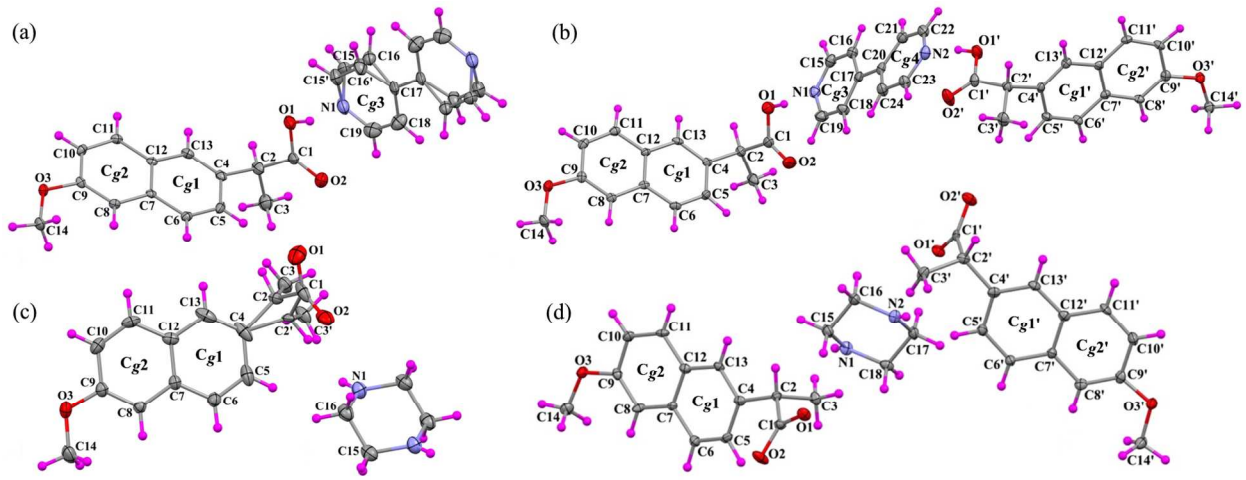

Fig. 2 ORTEP view of (a) *RS*-NPX–BPY, (b) *S*-NPX–BPY, (c) *RS*-NPX–PIZ and (d) *S*-NPX–PIZ with atom labelling scheme. Phenyl ring labelling code: C*g*1= C4-C5-C6-C7-C12-C13, C*g*2= C7-C8-C9-C10-C11-C12, C*g*3= N1-C15-C16-C17-C18 and C*g*4= N2-C22-C21-C20-C24-C23.

the Cambridge Crystallographic Data Centre and copies of the data can be obtained free of charge on application to CCDC, 12 Union Road, Cambridge CB2 1EZ, U.K. (fax: (+44)1223-336-033; e-mail: deposit@ccdc.cam.ac.uk; www: http://www.ccdc.cam.ac.uk).

In case of racemic cocrystals of *RS*-NPX–BPY (Fig. 2a) and *RS*-NPX–PIZ (Fig. 2c), the asymmetric unit consists of one NPX molecule and half molecule of BPY and PIZ, respectively, which are located on a crystallographic inversion centre. Also, the bipyridine molecules in *RS*-NPX–BPY (Fig. 2a) and the propionic acid side chain of naproxen in *RS*-NPX–PIZ (Fig. 2c) were disordered over two positions. In case of *S*-NPX-BPY (Fig. 2b) and *S*-NPX–PIZ (Fig. 2d), the asymmetric unit comprises of two independent *S*-NPX molecules and single molecules of BPY and PIZ, respectively.

Powder X-ray Diffraction (PXRD)

X-ray powder diffraction measurements were recorded on a Rigaku RINT diffractometer equipped with a Cu X-ray source operating at 40kV and 40mA and a secondary graphite monochromator allowing to select the Kα radiation of Cu (λ = 1.5418 Å). A scanning range of 2θ values from 2° to 42° at a scan rate of 2°/min was applied and the intensity of diffracted X-rays being collected at intervals of 0.01°. Variable temperature PXRD studies were carried out by mounting the sample in a high-temperature cell and heated at a rate of 5°C/min and stabilized for 10 min before each measurement.

Results and discussion

Crystal Structure

In NPX–BPY cocrystals, the naproxen and bipyridine molecules are linked together by O–H···N hydrogen bonds to form a centrosymmetric three component adduct in *RS*-NPX–BPY (Fig. 3a), whereas non-centrosymmetric adduct formation in *S*-NPX–BPY by the two asymmetric naproxen molecules with bipyridine

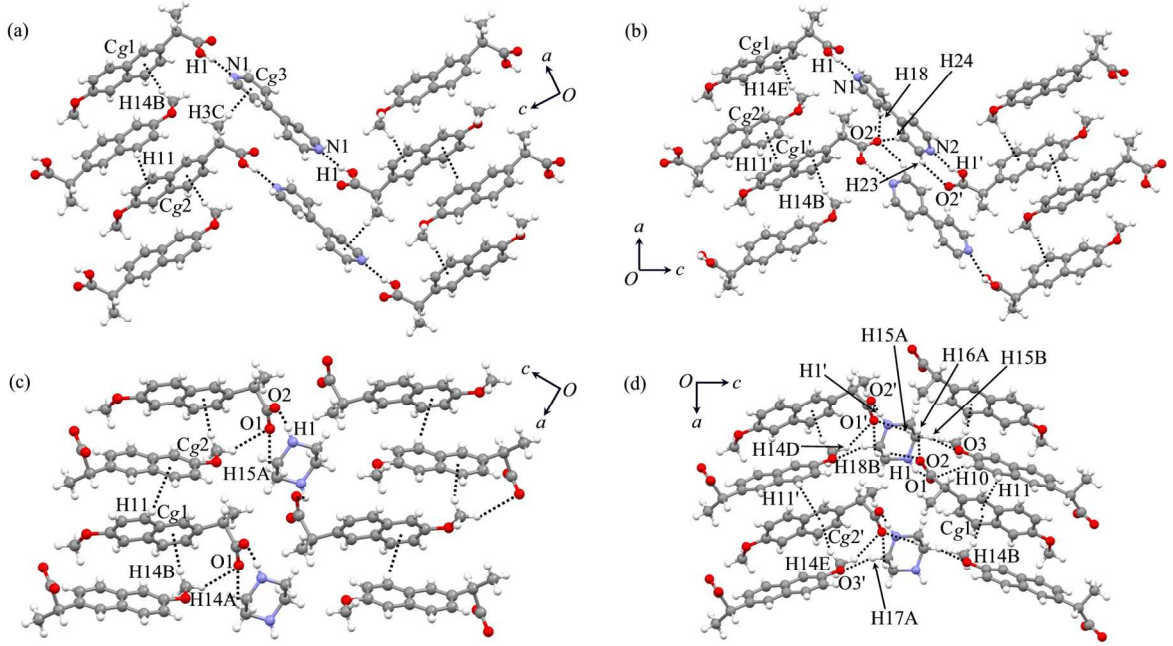

Fig. 3 Molecular packing consist of three components adducts in cocrystals of (a) *RS*-NPX–BPY, (b) *S*-NPX–BPY, (c) *RS*-NPX–PIZ and (d) *S*-NPX–PIZ viewing down the *b*-axis.

(Fig. 3b). These adducts were further linked by weak C–H···π interactions to form chains along the *c*-axis using C11–H11···C*g*2, C14–H14*B*···C*g*1 in *RS*-NPX–BPY, and C11–H11···C*g*2, C11'–H11'···C*g*2', C14–H14*B*···C*g*1' and C14'–H14*E*···C*g*1 in *S*-NPX–BPY (*see supporting information for all geometrical parameters*, Table ST1). Adjacent such chains were associated to form a herringbone molecular arrangement by C–H···π (C3–H3*C*···C*g*3) interactions in *RS*-NPX–BPY and weak bifurcated C–H···O interactions (C18–H18···O2' and C24–H24···O2') in *S*-NPX–BPY (Fig. 3a, 3b and Table ST1).

Isostructural three component adduct formation was also observed in NPX–PIZ cocrystals, in which the naproxen connected to the piperazine centrosymmetrically in *RS*-NPX–PIZ (Fig. 3c) and non-centrosymmetrically in *S*-NPX–PIZ (Fig. 3d) through O–H···N and C–H···O interactions (Table ST1). These molecular adducts were further linked to form a herringbone molecular arrangement by weak interactions such as C–H···π (C14–H14*B*···C*g*1, C11–H11···C*g*2 in *RS*-NPX–PIZ and C14–H14*B*···C*g*1, C11–H11···C*g*1, C14'–H14*E*···C*g*2', C11'–H11'···C*g*2' in *S*-NPX–PIZ) and C–H···O (C14–H14*A*···O1 in *RS*-NPX–PIZ and C10–H10···O1, C15–H15*B*···O3, C14'–H14*D*···O1', C17–H17*A*···O3' in *S*-NPX–PIZ) interactions (Fig. 3c, 3d and Table ST1).

Homochiral Molecular Organization

An interesting feature observed in the cocrystal of naproxen is the homochiral molecular organization of NPX molecules, which is the primary structural requirement for the occurrence of preferential enrichment.[14] Each three component adducts in the racemic crystals, that are composed of *R*-NPX (red colour in Fig. 4) and *S*-NPX (blue colour in Fig. 4) connected by bipyridine (green colour in Fig. 4a) in *RS*-NPX–BPY and piperazine (green colour in Fig 4c) in *RS*-NPX–PIZ, further linked by C–H···π interactions in such a way that the *R*-NPX (or *S*-NPX) molecules are associated to form a homochiral helical 1D *R*-NPX (or *S*-NPX) chains along the *a*-axis (Fig. 4a, 4c). In other words, *R*-NPX molecules were associated by C–H···π interactions to form homochiral 1D *R*-NPX chains and *S*-NPX molecules to

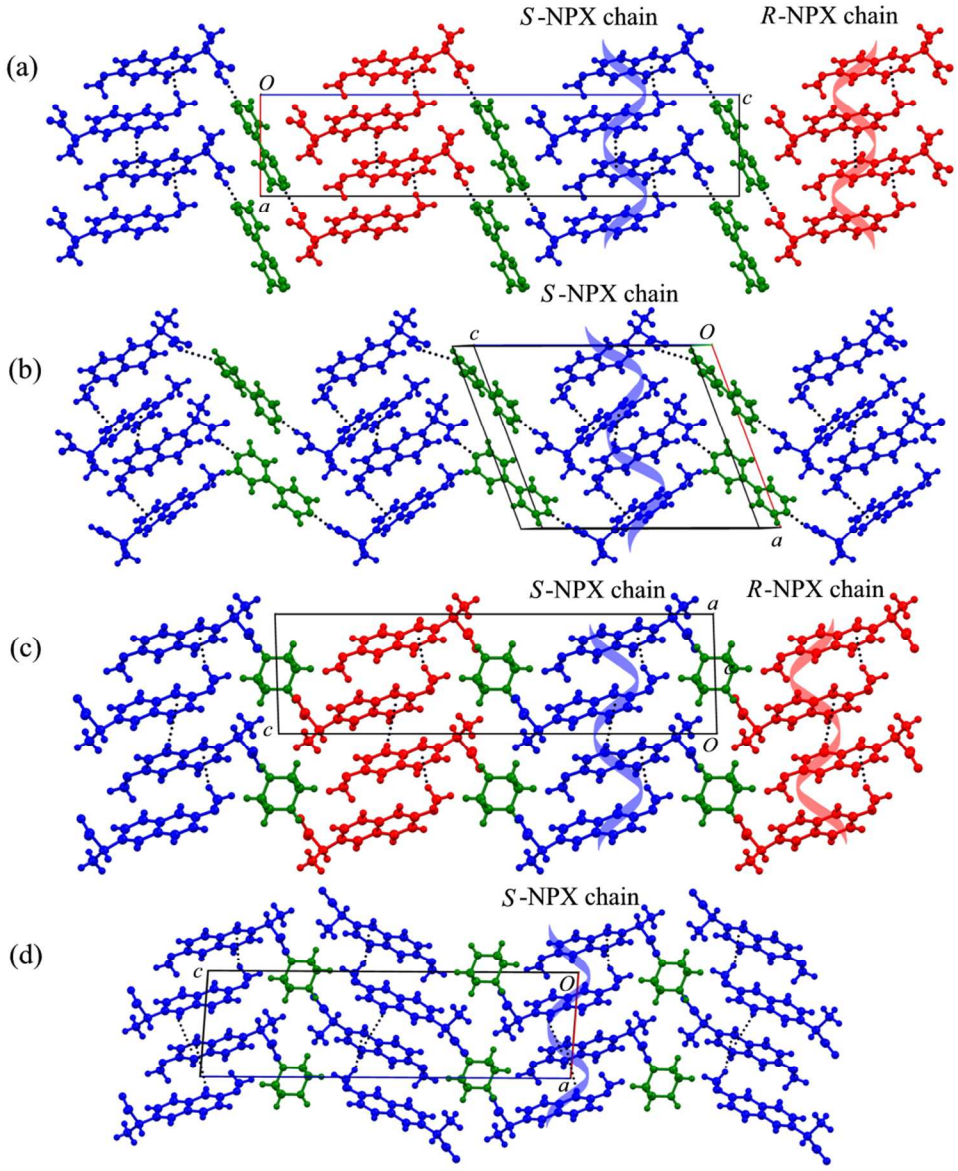

Fig. 4 Homochiral layer formation viewing down the *b*-axis in crystals of (a) *RS*-NPX-BPY, (b) *S*-NPX-BPY, (c) *RS*-NPX-PIZ and (d) *S*-NPX-PIZ.

homochiral 1D *S*-NPX chains, that are interconnected by bipyridine (Fig. 4a) or piperazine molecules (Fig. 4c). A similar type of homochiral NPX molecular chain formation was observed in case of their enantiomer cocrystals (*S*-NPX–BPY and *S*-NPX–PIZ), in which the naproxen molecules are associated *via* C–H···π interactions to form homochiral chains (two asymmetric *S*-NPX chains) and these chains further linked by bipyridine (Fig. 4b) and piperazine (Fig. 4d), respectively.

The naproxen molecules of trimeric units are further linked to the bipyridine by C18–H18···O2 contacts along the *b*-axis to form layers in *RS*-NPX–BPY. The overall molecular packing in the crystal lattice was resulted from the adjacent homochiral *R*-NPX and *S*-NPX chains that are linked by the bipyridine chains (*see supporting information*, Fig. SF2a). Similar packing was also observed in *S*-NPX-BPY with adjacent homochiral *S*-naproxen chains, that consists of two asymmetric *S*-NPX molecules, bound to bipyridine; however the molecules are associated with many intermolecular contacts such as C3–H3*C*···O1, C5–H5···O1 and C15–H15···O2, which led to a more close packing than that of its racemate (*see supporting information,* Fig. SF2b). In *RS*-NPX–PIZ cocrystals, naproxen molecule of the trimeric units binds to piperazine by C16–H16*B*···O1 contacts along the *b*-axis and are further linked to the adjacent naproxen by weak C16–H16*A*···O3 interaction to form layer (*see supporting information,* Fig. SF2c). In these layers also the overall packing is such that the adjacent homochiral naproxen chains are sand-witched by piperazine molecule. An isostructural molecular packing was also observed for *S*-NPX–PIZ; *i.e*. layer formation by the alternate homochiral *S*-naproxen chains and piperazine chains. However, these molecules were more closely bind with many intermolecular contacts namely C3'–H3*E*···O2', C5'–H5'···O2', C15–H15*B*···O3 and C17–H17*A*···O3' (*see supporting information,* Fig. SF2d).

Preferential Enrichment Studies of Naproxen Cocrystals

Recently, we have reported enantiomeric resolution of phenyl alanine-fumaric acid cocrystals using preferential enrichment phenomenon.[15] However, efficient enantiomeric resolution by preferential enrichment occurs only if the following five requirements[17] are satisfied; (i) unique crystal structures with homochiral 1D *R* and *S* chains, (ii) sufficient solubility difference (pure enantiomer >> racemate), (iii) occurrence of solid-to-solid polymorphic transition, (iv) selective re-dissolution of the excess enantiomer from the transformed crystals, and (v) eventual formation of non-racemic mixed crystals. We have succeeded in obtaining the desired molecular organization of NPX in cocrystals and carried out preferential enrichment studies. However, no efficient enrichment occurred due to the less solubility differences of the pure enantiomer than its racemates in various solvents; for example, solubilites of *S*-NPX–BPY, *RS*-NPX–BPY, *S*-NPX–PIZ and *RS*-NPX–PIZ in EtOH-H_2O (2:1) were found to be 32, 28, 7 and 6 mg/mL, respectively. In order to show good preferential enrichment, the solubility of pure enantiomer should be more than two times to the solubility of its racemate.

Phase Transformation Studies of NPX-BPY Cocrystals

Thermal Analysis by Differential Scanning Calorimetry (DSC)

The DSC plot of *S*-NPX–BPY crystals showed an endothermic peak at 96°C before the melting peak (119°C), indicating a probable phase transformation occurred during the heating (Fig. 5a). In order to study the thermal phase changes, repeated heating-cooling cycles of experiments were carried out for *S*-NPX–BPY crystals, which showed the additional endothermic peak (96°C) observed only in the first heating and the peak disappeared in the second (or third) heating. This could be due to the monotropic phase transformation of a metastable form to a stable form of cocrystal. Similarly, thermal studies of *RS*-NPX–BPY crystals were also carried out but no changes indicated during heating, whereas exothermic peaks were observed while cooling between 100-80°C (Fig. 5b).

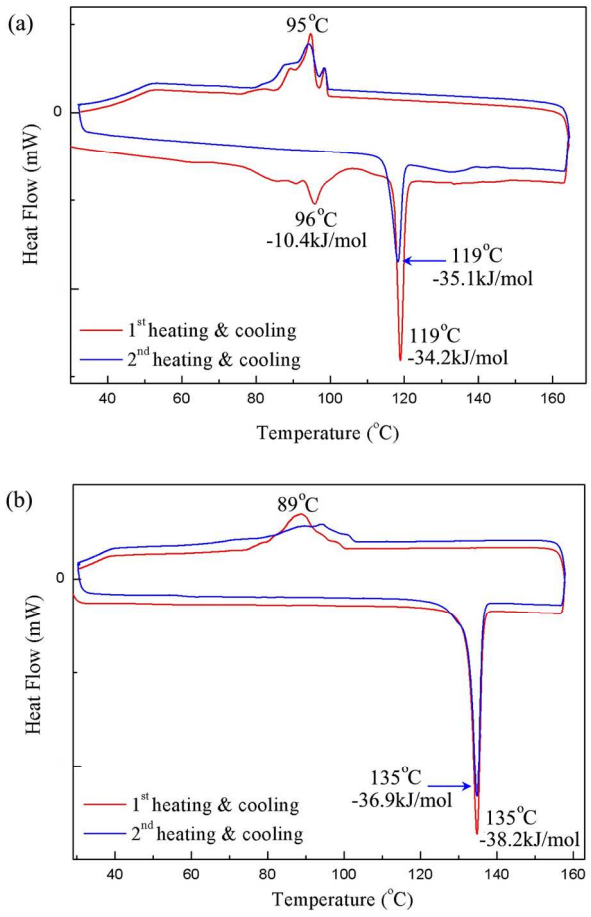

Fig. 5 DSC plots of heating-cooling cycles of naproxen–bipyridine cocrystals (a) *S*-NPX–BPY and (b) *RS*-NPX–BPY.

Hot Stage Microscopy (HSM) Studies

The DSC results of *S*-NPX-BPY crystals prompted us to study the phase transformation using HSM. Block cocrystals of NPX–BPY were slowly heated and cooled, and the images captured at each interval (Fig. 6). Transparent *S*-NPX–BPY crystal has become slowly opaque upon heating at 80°C onwards, but started a partial melting at 95-105°C, and then changed to a new phase, which was completely melted to liquid at 121°C (Fig. 6a). This indicates that a phase (polymorphic) transformation of cocrystal occurred upon heating. The slow cooling of the completely melted crystals, a polycrystalline phase started appearing at 105°C, almost solidified about 80°C, and finally produced a completely polycrystalline materials at room temperature. The

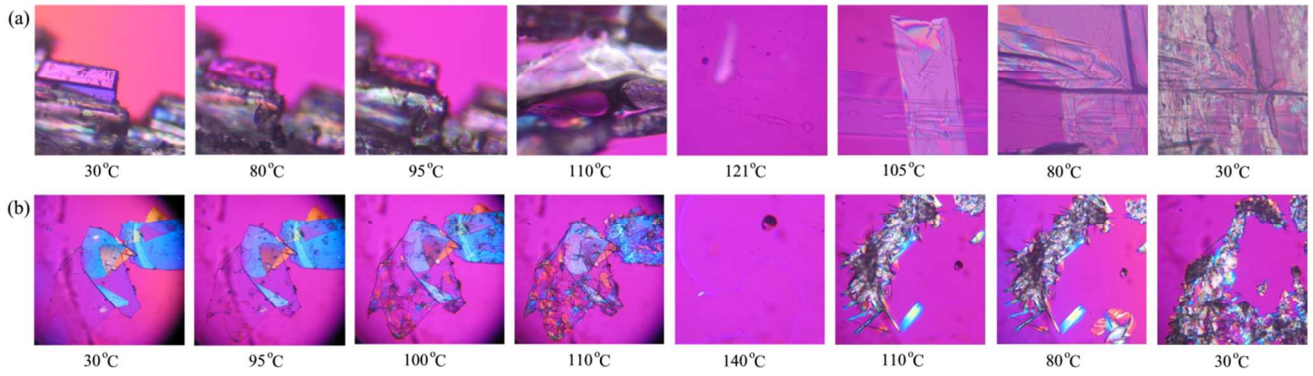

Fig. 6 Hot stage microscopic images of naproxen cocrystals captured under various temperatures (a) *S*-NPX–BPY and (b) *RS*-NPX–BPY.

second (or third) heating showed only one melting corresponds to the transformed *S*-NPX–BPY crystals, similar to that observed in the DSC plot (Fig. 5a).

Although we observed single melting peak for *RS*-NPX–BPY cocrystals (Fig. 5b), the HSM studies were carried out to check the probable phase transformation. Interestingly, the heating/cooling experiments of flat thin cocrystals indicated a certain type of phase changes upon heating and the images at each stage were captured (Fig. 6b). Upon slow heating, cracking of cocrystals were observed about 95°C onwards, partial melting between 105-115°C, and complete melting at 140°C. On slow cooling of the completely melted crystals, needle or block type polycrystals started appearing about 110°C and a completely polycrystalline materials were obtained at room temperature. The repeated heating (second or third) did not show partial melting and the observed complete melting corresponds to *RS*-NPX–BPY cocrystal. Although in the DSC plot of *RS*-NPX–BPY, the phase transformations upon heating were not observed (Fig. 5b), probably due to the small energy change that is not in the detectable level of the instrument.

High Temperature Powder X-ray Diffraction (HT-PXRD)

It has been clearly observed from the HSM studies that phase transformation occurs on heating and the transformed crystals are polycrystalline in nature. Therefore, we were unable to characterize the transformed crystal structure by SCXRD. We also tried to grow single crystals by seeding the transformed crystal into a supersaturated solution of NPX–BPY but failed to get suitable single crystals for SCXRD studies. Thus, the PXRD studies of *S*-NPX–BPY cocrystals were carried out by heating slowly and measured PXRD pattern at each intervals (Fig. 7a). We can see a slightly different pattern at 110°C in the first heating/cooling and also in the second heating and cooling. Similarly, in case of *RS*-NPX–BPY cocrystals, the new phase was not observed in the first heating but appeared in the first cooling (110°C), and also exhibited in the second heating/cooling (Fig. 7b). The new cocrystalline form is also confirmed by the FT-IR studies as explained below.

FT-IR Analysis

The thermally transformed cocrystalline phase is also characterized by the FT-IR studies in the solid state (KBr pellet). The IR spectra before and after the phase transformations of NPX–BPY cocrystals are almost identical, indicating the existence of cocrystals rather than decomposition of their individual crystals. Transformed NPX-BPY cocrystals are also

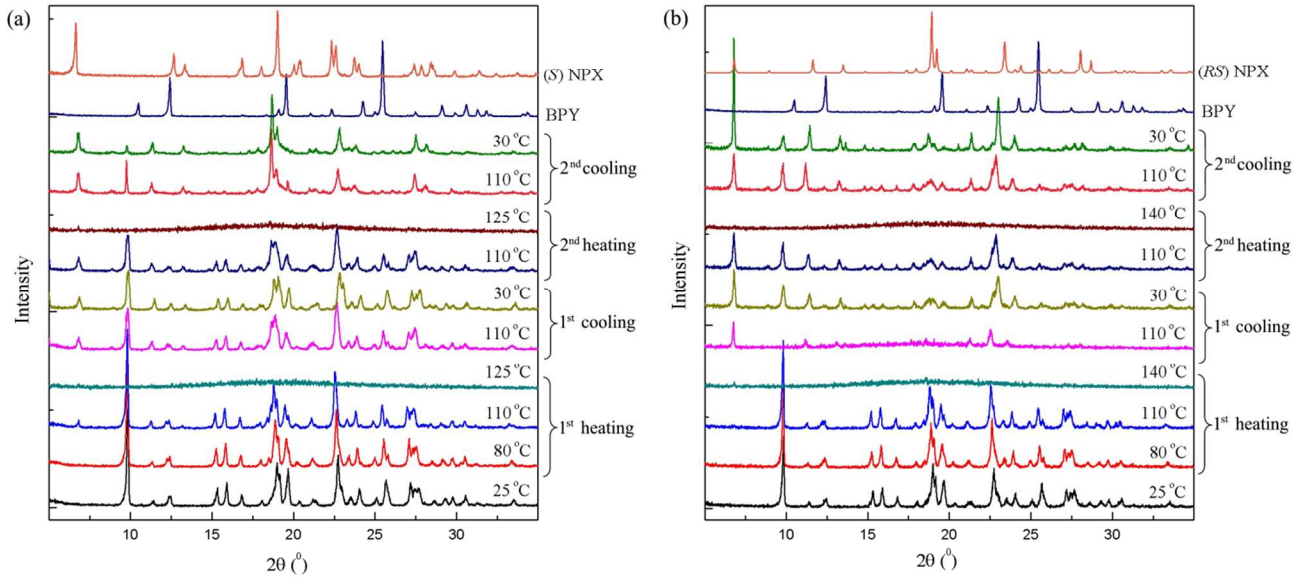

Fig. 7 Variable temperature PXRD plots of heating-cooling cycles of (a) *S*-NPX–BPY and (b) *RS*-NPX–BPY cocrystals

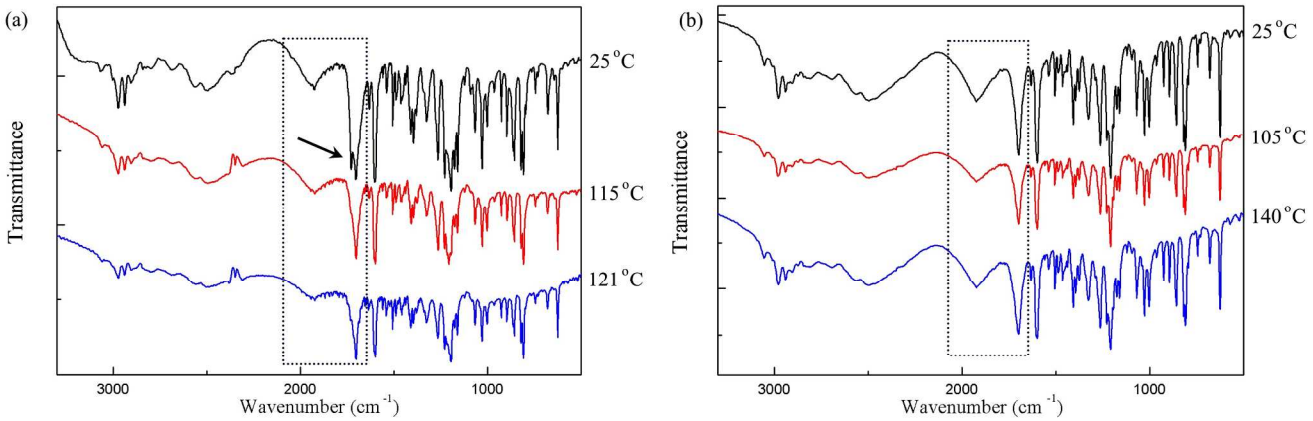

Fig. 8 FT-IR plots transformed cocrystals of (a) *S*-NPX–BPY and (b) *RS*-NPX–BPY. Dotted box indicates the IR spectral band for the acid-pyridine synthon in cocrystals.[24] Arrow indicates C=O doublets for the *S*-NPX–BPY cocrystals.

confirmed by the IR spectral marker (1600/1900-2400 cm^{-1}) for the acid-pyridine synthon in cocrystals.[24] It is interesting to note that the stretching band of C=O group in *S*-NPX–BPY cocrystals was doublets initially and it has become singlet in the transformed crystals (Fig. 8a). This can be correlated with the number of asymmetric molecules in the naproxen-bipyridine cocrystals; *i.e*. carboxylic acid groups of the two asymmetric *S*-NPX molecules (Fig. 3b) that are differently linked to the bipyridine in *S*-NPX–BPY cocrystals resulted C=O doublets in the IR spectra (arrow showed in Fig. 8a), whereas after thermal phase transformation it has becomes C=O singlet probably due to the symmetric organization of *S*-NPX molecules similar to that observed in the racemate (Fig. 8b). The knowledge of multiple molecules (number of asymmetric units) in a given crystal is very important for the crystal structure prediction and makes it more difficult to predict polymorphs.[25]

confirmed by the IR spectral marker (1600/1900-2400 cm^{-1}) for the acid-pyridine synthon in cocrystals.[24] It is interesting to note that the stretching band of C=O group in *S*-NPX–BPY cocrystals was doublets initially and it has become singlet in the transformed crystals (Fig. 8a). This can be correlated with the number of asymmetric molecules in the naproxen-bipyridine cocrystals; *i.e*. carboxylic acid groups of the two asymmetric *S*-NPX molecules (Fig. 3b) that are differently linked to the bipyridine in *S*-NPX–BPY cocrystals resulted C=O doublets in the IR spectra (arrow showed in Fig. 8a), whereas after thermal phase transformation it has becomes C=O singlet probably due to the symmetric organization of *S*-NPX molecules similar to that observed in the racemate (Fig. 8b). The knowledge of multiple molecules (number of asymmetric units) in a given crystal is very important for the crystal structure prediction and makes it more difficult to predict polymorphs.[25]

Conclusions

We have succeeded in obtaining the desired homochiral 1D molecular structure of naproxen essential to induce preferential enrichment by crystal engineering technique. Cocrystals of racemic and *S*-naproxen (NPX) with bipyridine (BPY) and piperazine (PIZ) were prepared and the crystal structure analysis showed the presence of homochiral NPX chain formation using weak intermolecular C–H···π interactions. The monotropic polymorphic transformation of NPX–BPY cocrystals occurred upon heating and the new phase was characterized by DSC, PXRD, hot-stage microscopy and FT-IR spectroscopy. The polymorphic transformation studies are very important in the pharmaceutical industry due to the different physico-chemical properties of API.

Acknowledgements

This work was supported by the Grant-in-Aid for Scientific Research (No. 23245008) from Japan Society for the Promotion of Science.

References

1 (a) G. R. Desiraju, *Crystal Engineering:The Design of Organic Solids*, Elsevier, Amsterdam, 1989; (b) K. R. Seddon and M. Zaworotko, *Crystal engineering: the design and application of functional solids*, Kluwer Academic Publishers, Netherlands, 1996; (c) D. Braga and F. Grepioni, *Making Crystals By Design: Methods, Techniques and Applications*, Wiley-VCH, Weinheim, 2007; (d) C. B. Aakeroy, N. R. Champness and C. Janiak, *CrystEngComm*, 2010, **12**, 22; (e) J. M. Thomas, *CrystEngComm*, 2011, **13**, 4304; (f) G. R. Desiraju, J. J. Vittal and A. Ramanan, *Crystal Engineering: A Textbook*, World Scientific, Singapore, 2011; (g) A. Bacchi, M. Carcelli and P. Pelagatti, *Crystallogr. Rev.*, 2012, **18**, 253; (h) G. R. Desiraju, *J. Am.Chem.Soc.,* 2013, **135**, 9952.

2 (a) E. R. T. Tiekink, J. Vittal, M. Zaworotko, *Organic Crystal Engineering: Frontiers in Crystal Engineering*, Wiley-VCH, Weinheim, 2010; (b) A. Lemmerer, C. Esterhuysen and J. Bernstein, *J. Pharm. Sc*., 2010, **99**, 4054; (c) H. G. Brittain, *Cryst. Growth Des*., 2011, **12**, 1046; (d) N. J. Babu, P. Sanphui and A. Nangia, *Chem. Asian J.,* 2012, **7**, 2274.

3 (a) J. Wouters and L. Quere, *Pharmaceutical Salts and Co-crystals*, Royal Society of Chemistry, Cambridge, UK, 2011; (b) S. Aitipamula, R. Banerjee, A. K. Bansal, K. Biradha, M. L. Cheney, A. R. Choudhury, G. R. Desiraju, A. G. Dikundwar, R. Dubey, N. Duggirala, P. P. Ghogale, S. Ghosh, P. K. Goswami, N. R. Goud, R. R. K. R. Jetti, P. Karpinski, P. Kaushik, D. Kumar, V. Kumar, B. Moulton, A. Mukherjee, G. Mukherjee, A. S. Myerson, V. Puri, A. Ramanan, T. Rajamannar, C. M. Reddy, N. Rodriguez-Hornedo, R. D. Rogers, T. N. G. Row, P. Sanphui, N. Shan, G. Shete, A. Singh, C. C. Sun, J. A. Swift, R. Thaimattam, T. S. Thakur, R. K. Thaper, S. P. Thomas, S. Tothadi, V. R. Vangala, N. Variankaval, P. Vishweshwar, D. R. Weyna and M. J. Zaworotko, *Cryst. Growth Des*., 2012, **12**, 2147 ; (c) J. W. Steed, *Trends Pharmcol. Sci.,* 2013, **34**, 185.

4 (a) J. Good and N. Rodriguez-Hornedo, *Cryst. Growth Des*., 2009, **9**, 2252; (b) C. B. Aakeroy, S. Forbes and J. Desper, *J. Am. Chem. Soc*., 2009, **131**, 17048; (c) G. Bolla, P. Sanphui and A. Nangia, *Cryst. Growth Des*., 2013, **13**, 1988; (d) S. Ghosh and C. M. Reddy, *CrystEngComm*, 2011, **13**, 5650

5 (a) G. R. Desiraju and T. Steiner, *The Weak Hydrogen Bond in Structural Chemistry and Biology*, Oxford University Press, New York,1999; (b) L. J. Prins, D. N. Reinhoudt and P. Timmerman, *Angew. Chem. Int. Ed.,* 2001, **40**, 2382; (c) A. Lemmerer and J. Bernstein, *CrystEngComm*, 2010, **12**, 2029; (d) A. Delori, P. T. A. Galek, E. Pidcock, M. Patni, W. Jones, *CrystEngComm*, 2013, **15**, 2916.

6 (a) P. Metrangolo, H. Neukirch, T. Pilati, G. Resnati, *Acc. Chem. Res*., 2005, **38**, 386; (b) R. G. Gonnade, M. S. Shashidhar, M. M. Bhadbhade, *J. Indian Inst. Sci.* 2007, **87**, 149; (c) P. Metrangolo, G. Resnati, *Halogen Bonding: Fundamentals and Applications, Structure and Bonding*, Springer-Verlag, Berlin, 2008; (d) D. Chopra and T. N. G. Row, *CrystEngComm*, 2011, **13**, 2175.

7 (a) K. Manoj, R. G. Gonnade, M. M. Bhadbhade and M. S. Shashidhar, *Acta Crystallogr., Sect. C*: *Cryst. Struct. Commun*., 2007, **63**, o555; (b) K. Manoj, R. G. Gonnade, M. M. Bhadbhade and M. S. Shashidhar, *CrystEngComm*, 2009, **11**, 1022; (c) M. R. Chierotti and R. Gobetto, *CrystEngComm*, 2013, **15**, 8599.

8 (a) Nishio, M. *Phys. Chem. Chem. Phys.* 2011, **13**, 13873; (b) R. Bishop, *Aus. J. Chem*., 2012, **65**, 1361; (c) S. Ghosh, A. Mondal, M. S. R. N. Kiran, U. Ramamurty and C. M. Reddy *Cryst. Growth Des*., 2013, **13**, 4435.

9 (a) Mullin, J. W. *Crystallization*, Heinemann-Butterworth, London, 1993; (b) T. Threlfall, *Org. Process Res. Dev*., 2000, **4**, 384; (c) K. Fucke, S. A. Myz, T. P. Shakhtshneider, E. V. Boldyreva and U. J. Griesser, *New J. Chem.*, 2012, **36**, 1969; (d) K. Manoj, R. G. Gonnade, M. M. Bhadbhade and M. S. Shashidhar, *CrystEngComm*, 2012, **14**, 1716.

10 (a) C. Butterhof, K. Barwinkel, J. Senker and J. Breu, *CrystEngComm*, 2012, **14**, 6744; (b) 30 S. L. James, C. J. Adams, C. Bolm, D. Braga, P. Collier, T. Friscic, F. Grepioni, K. D. M. Harris, G. Hyett, W. Jones, A. Krebs, J. Mack, L. Maini, A. G. Orpen, I. P. Parkin, W. C. Shearouse, J. W. Steed and D. C. Waddell, *Chem. Soc. Rev*., 2012, **41**, 413; (c) H. Morrison, M. Mrozek-Morrison, J. Toschi, V. Luu, H. Tan, and D. Daurio, *Org. Process Res. Dev*., 2013, **17**, 533.

11 (a) P. Bag, M. Patni and C. M. Reddy, *CrystEngComm*, 2011, **13**, 5650; (b) K. Manoj, R. G. Gonnade, M. S. Shashidhar and M. M. Bhadbhade, *CrystEngComm*, 2012, **14**, 1716.

12 T. Friscic and W. Jones, *Cryst. Growth Des*., 2009, **9**, 1621.

13 (a) P. G. Karamertzanis, A. V. Kazantsev, N. Issa, G. W. A. Welch, C. S. Adjiman, C. C. Pantelides and S. L. Price, *J. Chem. Theory Comput.*, 2009, **5**, 1432; (b) H. C. S. Chan, J. Kendrick, M. A. Neumannc and F. J. J. Leusen, *CrystEngComm*,2013, **15**, 3799.

14 (a) R. Tamura and T. Ushio, *Enantiomer Separation*: *Fundamentals and Practical Methods*, ed. F. Toda, Kluwer Academic Publishers, Dordrecht, The Netherlands, 2004; (b) R. Tamura, H. Takahashi, D. Fujimoto and T. Ushio, *Top. Curr. Chem*., 2007, **269**, 53; (c) S. Iwama, M. Horiguchi, H. Sato, Y. Uchida, H. Takahashi, H. Tsue and R. Tamura, *Cryst. Growth Des*., 2010, **10**, 2668; (d) R. Tamura, S. Iwama and R. G. Gonnade, *CrystEngComm*, 2011, **13**, 5269.

15 R. G. Gonnade, S. Iwama, Y. Mori, H. Takahashi, H. Tsue and R. Tamura, *Cryst. Growth Des*., 2011, **11**, 607.

16 R. G. Gonnade, S. Iwama, R. Sugiwake, K. Manoj, H. Takahashi, H. Tsue and R. Tamura. *Chem. Commun*., 2012, **48**, 2791.

17 R. Tamura, S. Iwama and H. Takahashi, *Symmetry*, 2010, **2**, 112.

18 P. J. Harrington, E. Lodewijk, *Org. Process. Res. Dev*., 1997, **1**, 72.

19 D. E. Braun, M. Ardid-Candel, E. D'Oria, P. G. Karamertzanis, J. B. Arlin, A. J. Florence, A. G. Jones and S. L. Price, *Cryst. Growth Des*., 2011, **11**, 5659.

20 *CrystalStructure 3.8*: Crystal Structure Analysis Package; Rigaku and Rigaku Americas (2000–2007), 9009 New Trails Dr., The Woodlands,TX 77381, USA.

21 A. Altomare, M. Burla, M. Camalli, G. Cascarano, C. Giacovazzo, A. Guagliardi, A. Moliterni, G. Polidori and R. Spagna, *J. Appl. Crystallogr.*, 1999, **32**, 115.

22 G. M. Sheldrick, *Acta Crystallogr., Sect. A*: *Found. Crystallogr.*, 2008, **64**, 112.

23 C. F. Macrae, I. J. Bruno, J. A. Chisholm, P. R. Edgington, P. McCabe, E. Pidcock, L. Rodriguez-Monge, R. Taylor, J. van de Streek and P. A. Wood, *J. Appl. Cryst*., 2008, **41**, 466.

24 A. Mukherjee, S. Tothadi, S. Chakraborty, S. Ganguly and G. R. Desiraju, *CrystEngComm*, 2013, **15**, 4640.

25 (a) G. Day, *Crystallogr. Rev.*, 2011, **17**, 3; (b) S. L. Price, *Acta Cryst.*, 2013, **B69**, 313.

Graphical Abstract

Crystal Engineering of Homochiral Molecular Organization of Naproxen in Cocrystals and Their Thermal Phase Transformation Studies

K. Manoj,* Rui Tamura, Hiroki Takahashi and Hirohito Tsue

Crystal engineering principles were used to produce the homochiral *R*- and *S*-chains of naproxen (NPX) by cocrystallization with bipyridine (BPY) and piperazine (PIZ).